Kinetics of fluorine atoms in high-density carbon–tetrafluoride plasmas

K. Sasaki,[a] Y. Kawai, C. Suzuki, and K. Kadota
Department of Electronics, Nagoya University, Nagoya 464-01, Japan

(Received 5 May 1997; accepted for publication 11 September 1997)

Reaction processes of fluorine (F) atoms in high-density carbon–tetrafluoride (CF_4) plasmas were investigated using vacuum ultraviolet absorption spectroscopy. A scaling law $n_F \propto (n_e n_{CF_4})^{0.5-0.7}$ was found experimentally, where n_F is the F atom density and n_e and n_{CF_4} stand for the electron and parent gas (CF_4) densities, respectively. The lifetime measurement in the afterglow showed that the decay curve of the F atom density was composed of two components: a rapid decay in the initial afterglow and an exponential decrease in the late afterglow. The decay time constant in the initial afterglow τ_1 satisfied the scaling law $\tau_1 \propto (n_e n_{CF_4})^{-(0.3-0.4)}$, which is a consistent relationship with the scaling law for the F atom density. The two scaling laws and the lifetimes of CF_x radicals suggest that the major loss process of F atoms in the initial afterglow is the reaction with CF_x radicals (probably, $x=3$) on the wall surface. The loss process in the late afterglow was simple diffusion to the wall surface. The surface loss probability of F atoms on the chamber wall was evaluated from the decay time constant in the late afterglow, and was on the order of 10^{-3}.
 [S0021-8979(97)02824-7]

I. INTRODUCTION

Fluorine (F) atoms are the major etchant for Si and SiO_2. In the fabrication of ultralarge-scale integrated (ULSI) circuits, small contact holes (<0.25 μm in diameter) are bored through SiO_2 thin films by dry etching using fluorocarbon plasmas.[1,2] In this process, high etching selectivity (>20) of SiO_2 over underlying Si is required. When conventional parallel-plate rf plasma sources with low electron densities ($\sim 10^{10}$ cm^{-3}) are used, the sufficiently high etching selectivity has been obtained rather easily. However, the parallel-plate plasma sources operated under high gas pressures (>100 mTorr) have a limitation for the high etching anisotropy since the trajectories of positive ions are distorted by collisions with neutral molecules during passing through the ion sheath in front of the substrate.[3] To obtain anisotropic etching of the high-aspect-ratio pattern, various high-density ($>10^{11}$ cm^{-3}) plasma sources operated under low gas pressures (<10 mTorr) have recently been developed, such as electron cyclotron resonance (ECR) plasmas,[3,4] inductively coupled plasmas (ICPs),[5] and helicon-wave excited plasmas.[6] The principal problem in SiO_2 etching using these high-density plasma sources is the low etching selectivity.[4,7] Both Si and SiO_2 are etched by F atoms, while CF_x radicals are the precursors of polymerization which detract the etching rate of Si. Hence the etching selectivity is considered to be sensitive to the density ratio of CF_x radicals to F atoms in plasmas.[8] In the high-density plasma sources, the densities of highly dissociated species are higher than those in the conventional parallel-plate plasma sources, resulting in the low etching selectivity.

To achieve SiO_2 etching with the high rate, the high anisotropy, and the high selectivity, the control of the neutral radical densities in fluorocarbon plasmas is the most important issue. The neutral radical densities in plasmas are determined as a result of complicated reactions among parent gas, neutral radicals, reactive ions, and electrons. Hence the knowledge of the reaction kinetics of the above species is required for the control of the composition of CF_x radicals and F atoms in fluorocarbon plasmas. For the measurements of the CF_x radical densities, various methods such as laser-induced fluorescence (LIF) spectroscopy,[9] infrared laser absorption spectroscopy (IRLAS),[10] and appearance mass spectrometry (AMS)[11] have been developed. These diagnostics provide useful information on the reaction kinetics of CF_x radicals in fluorocarbon plasmas. Contrary to this, the F atom density is extensively measured by the actinometry technique,[12] which can provide only the relative F atom density under the following assumptions:

(1) all the excited states of F atoms originate from the atomic ground state, and
(2) the excitation cross sections have the same energy dependence for both F and the actinometer atoms (usually Ar).

In addition, the lifetime measurement of F atoms in the afterglow is impossible by actinometry since no emission can be obtained. The lifetime measurement is a useful method for the investigation of loss processes of reactive species. Recently, we have developed vacuum ultraviolet absorption spectroscopy (VUVAS) for the absolute density measurements of F atoms in fluorocarbon plasmas.[13] In the present study, we have adopted this method to high-density CF_4 plasmas excited by helicon-wave discharges to study the reaction kinetics of F atoms. According to the reaction cross sections available to date,[14,15] the major production process of F atoms in CF_4 plasmas is dissociative ionization of the parent gas by electron impact ($CF_4 + e \rightarrow CF_3^+ + F + 2e$). Hence, in the present work, we emphasize the loss processes of F atoms which can be understood from the density and lifetime measured by VUVAS.

[a]Electronic mail: sasaki@nuee.nagoya-u.ac.jp

 0021-8979/97/82(12)/5938/6/$10.00

II. EXPERIMENT

The apparatus of the present experiments is the same as that described in a previous paper.[13] The high-density CF_4 plasmas were produced by helicon-wave discharges in a linear machine with a uniform magnetic field of 1 kG along the cylindrical axis of the vacuum chamber. Various rf powers at 13.56 MHz were applied to an $m=1$ helical antenna wound around a quartz glass tube 3 cm in diameter.[16] The vacuum chamber was composed of a Pyrex glass tube (9 cm in diameter) and two stainless-steel observation chambers ($20\times20\times10$ cm). Pure CF_4 gas was used for discharges with a fixed gas flow rate of 4.4 ccm. The gas pressure was varied by changing the pumping speed. The plasmas were produced periodically with a repetition rate of 4 Hz and a discharge duration of 10 ms.

The absolute F atom density was measured by VUVAS in the down stream plasma at a distance of approximately 50 cm from the end of the helical antenna. In VUVAS,[13] a compact ECR CF_4 plasma device operated under a low microwave power (0.1 kW) and a low gas pressure (1 mTorr) was employed as the light source in the VUV wavelength range. The wavelength of the probe emission for detecting F atoms at the ground state ($2p^{52}P^{\circ}$) was 95.85 nm which was obtained by the transition between $3s^2P_{3/2}$ and $2p^5\,{}^2P^{\circ}_{1/2}$ states. By differentially pumping the vacuum tube connecting the helicon plasma to the ECR plasma to prevent neutral radicals from passing through, an absorption spectroscopy system with no vacuum windows was constructed. The absorption length was 36 cm which was much longer than the diameter of the plasma column (3 cm). Since the lifetime of F atoms was much longer than the geometrical diffusion time determined by the chamber design, a uniform distribution was assumed for the F atom density in the helicon chamber along the transmission line of the probe emission. The absolute F atom density was deduced from the absorption with a conventional theory[17] by assuming Doppler broadening at a temperature of 400 K for the spectral distribution of the probe emission. Doppler broadening at 300 K was assumed for the spectral distribution of absorbing F atoms in the helicon chamber, since most of the F atoms were placed outside of the plasma column. The transition probability of $1.3\times10^8\ s^{-1}$ was used to evaluate the absorption cross section.[18] A small error within a factor of 2 was expected for the absolute F atom density by evaluating various sources of error. For the measurements of the electron density, a microwave interferometer at 35 GHz was installed at 10 cm upper stream from the observation chord of VUVAS.

III. RESULTS

Figure 1 shows the absolute F atom density measured by VUVAS. In Fig. 1(a), the F atom density was measured for various rf powers with a fixed gas pressure of 5 mTorr, while in Fig. 1(b), the F atom density was examined as a function of the CF_4 gas pressure for a fixed rf power of 1 kW. The F atom densities plotted in Fig. 1 were observed at a discharge time of 9.9 ms when both the electron density and the neutral radical densities including F atoms roughly reached their quasi-steady-state values. As has been reported in the previous paper,[13] the F atom density was on the order of $10^{12}-10^{13}\ cm^{-3}$. Considering the results of laser-induced fluorescence spectroscopy for a CF_4 pressure of 30 mTorr,[19] the CF radical density for the discharge conditions similar to those in the present experiments may be on the order of $10^{11}\ cm^{-3}$. The increase in the F atom density with the rf power is due to the increase in the electron density. On the other hand, the decrease in the F atom density with the CF_4 pressure is attributed mainly to the lower electron density for the higher gas pressure. In our helicon-wave CF_4 plasmas, a higher electron density can be obtained for a higher rf power and a lower gas pressure. This may be because the excitation efficiency of the helicon wave decreases with the CF_4 gas pressure.[20]

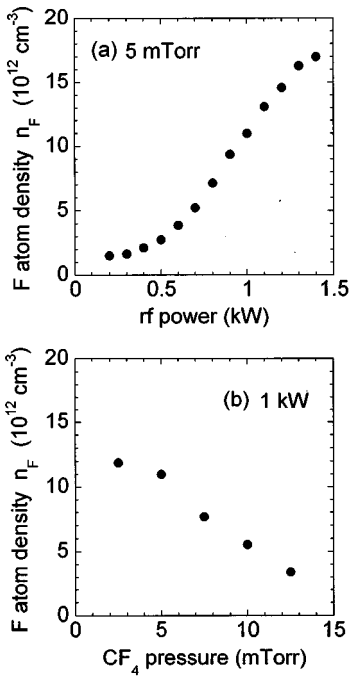

FIG. 1. Absolute F atom density measured by vacuum ultraviolet absorption spectroscopy as a function of (a) the rf power and (b) the CF_4 gas pressure. The CF_4 pressure was fixed at 5 mTorr in (a) and the rf power was fixed at 1 kW in (b).

The measurement of the F atom density was repeated for various rf powers and CF_4 gas pressures. The F atom densities at 9.9 ms are summarized in Fig. 2 as a function of the product between the electron density n_e and the density of the parent gas n_{CF_4}. Since the major production process of F atoms is dissociative ionization of CF_4 by electron impact, the horizontal axis of Fig. 2 is proportional to the production rate of F atoms. The plots indicated by the same symbol correspond to the F atom densities obtained for a fixed CF_4 gas pressure and various rf powers from 0.2 to 3 kW. The electron density was measured by the microwave interferometer. The electron density at the observation position of VUVAS may roughly be the same as that measured by the microwave interferometer because of the strong magnetic field and the low gas pressures. The density of the parent gas was calculated from the filled CF_4 gas pressure. The decrease in n_{CF_4} due to dissociation was not taken into consideration.

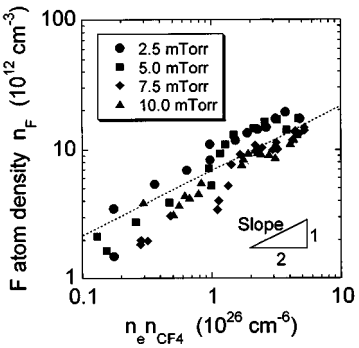

FIG. 2. The absolute F atom density n_F as a function of the product between the electron density n_e and the density of the parent gas n_{CF_4}. The dotted curve illustrated in the figure shows a relationship $n_F \propto (n_e n_{CF_4})^{0.5}$.

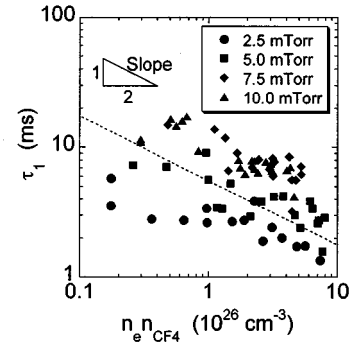

FIG. 4. The decay time constant of the F atom density in the initial afterglow τ_1 as a function of the product between the electron and parent gas densities $n_e n_{CF_4}$. The dotted curve illustrated in the figure shows a relationship $\tau_1 \propto (n_e n_{CF_4})^{-0.5}$.

The maximum dissociation degree of CF_4 in the present experiments was approximately 25% for a CF_4 pressure of 2.5 mTorr and $n_F \simeq 2\times 10^{13}$ cm^{-3}. As shown in Fig. 2, the F atom density was essentially determined by $n_e n_{CF_4}$. By applying the least squares method to each data set for fixed gas pressures, a relationship

$$n_F \propto (n_e n_{CF_4})^{0.5-0.7} \tag{1}$$

was evaluated from the experimental results, where n_F denotes the F atom density. The dotted curve illustrated in Fig. 2 shows the relationship $n_F \propto (n_e n_{CF_4})^{0.5}$.

To understand the loss processes of F atoms in the high-density CF_4 plasma, we carried out the lifetime measurement of the F atom density in the afterglow. A typical temporal variation of the F atom density is shown in Fig. 3. The rf power and the CF_4 gas pressure were 1.5 kW and 5 mTorr, respectively. The rf power was turned off at $t=10$ ms. After the termination of the rf power, the F atom density dropped rapidly during ~ 4 ms with a decay time constant of $\tau_1 \simeq 3.4$ ms. After that, the F atom density decreased exponentially with a decay time constant of $\tau_2 \simeq 27$ ms. The error in the evaluation of the former decay time constant τ_1 may be rather large since the duration of the initial density decay is comparable to τ_1. In the present helicon-wave CF_4 plasmas, decay time constants less than 20 μs were observed for the electron density.[21] The decay time constants of the CF and CF_2 radical densities were examined by laser-induced fluorescence spectroscopy, and were ~ 0.3 ms and ~ 5 ms, respectively, for an rf power of 1 kW and a CF_4 pressure of 5 mTorr.[22]

The decay time constant τ_1 in the initial afterglow is summarized in Fig. 4 as a function of $n_e n_{CF_4}$. Similar to Fig. 2, plots indicated by the same symbol were obtained for various rf powers and fixed gas pressures. Although the data points obtained experimentally include somewhat large scatter, the following two tendencies can be seen from the figure:

(1) τ_1 decreases with $n_e n_{CF_4}$, and
(2) τ_1 is longer for the higher gas pressure.

By applying the least squares method, the following relationship

$$\tau_1 \propto (n_e n_{CF_4})^{-(0.3-0.4)} \tag{2}$$

was roughly evaluated between τ_1 and $n_e n_{CF_4}$. In the figure, a relationship $\tau_1 \propto (n_e n_{CF_4})^{-0.5}$ is illustrated by the dotted curve.

The decay time constant τ_2 in the late afterglow was not dependent on the rf power but was strongly dependent on the CF_4 gas pressure. Hence no particular relationships were found between τ_2 and $n_e n_{CF_4}$. Figure 5 shows the CF_4 pres-

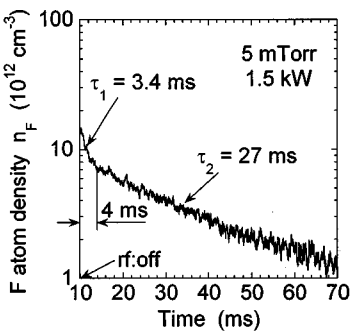

FIG. 3. Temporal variation of the F atom density in the afterglow. The rf power and the CF_4 gas pressure were 1.5 kW and 5 mTorr, respectively.

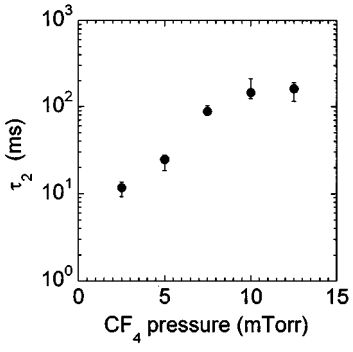

FIG. 5. Pressure dependence of the decay time constant of the F atom density in the late afterglow τ_2. The solid circles represent the averages of the decay time constants for various rf powers. The error bars correspond to the maximum and minimum values obtained during the power scan.

sure dependence of the decay time constant τ_2. The solid circles correspond to the averages of τ_2 observed for various rf powers from 0.2 to 3 kW. The maximum and minimum values of τ_2 obtained during the power scan are indicated by the error bars. As shown in the figure, τ_2 increased steeply with the CF_4 pressure in the range of 2.5–10 mTorr, and was much longer than the decay time constant τ_1 in the initial afterglow.

IV. DISCUSSION

According to the cross section data shown in the literature,[14,15] the dominant reaction of CF_4 with electrons is dissociative ionization,

$$CF_4+e\rightarrow CF_3^+ +F+2e. \tag{3}$$

Hence F atoms are mainly produced by Eq. (3), and other multistep reactions such as $CF_3+e\rightarrow CF_2+F+e$ are negligible. Accordingly, the behavior of the F atom density can be understood by the following simplified rate equation:

$$\frac{dn_F}{dt}=k_p n_e n_{CF_4}-\left(\frac{1}{\tau_D}+\frac{1}{\tau_R}\right)n_F=k_p n_e n_{CF_4}-\frac{n_F}{\tau}, \tag{4}$$

where k_p is the reaction rate coefficient for dissociative ionization shown in Eq. (3), τ_D denotes the diffusion time constant of F atoms, τ_R stands for the decay time constant of F atoms due to reactions, and $1/\tau=1/\tau_D+1/\tau_R$. The diffusion time constant τ_D is given by[23]

$$\tau_D=\frac{\Lambda_0^2}{D}+\frac{2l_0(2-\alpha)}{\overline{v}\,\alpha}, \tag{5}$$

where D denotes the diffusion coefficient, Λ_0 is the geometrical diffusion length determined by the chamber design, $l_0=V/S$ with V and S being the volume and surface area of the chamber, respectively, $\overline{v}$ is the mean velocity of F atoms given by $\sqrt{8kT/\pi M}$ (T and M are the temperature and mass of F atoms, respectively, and k is the Boltzmann constant), and α stands for the surface loss probability on the chamber wall. When the surface loss probability equals unity, Eq. (5) gives the geometrical diffusion time which is calculated as $\Lambda_0^2/D+2l_0/\overline{v}\simeq 0.16$ ms for a CF_4 gas pressure of 2.5 mTorr theoretically.[24] On the other hand, the second term of the right hand side of Eq. (5) dominates the first one if the surface loss probability is much smaller than unity. In this case, the diffusion time constant τ_D becomes independent of the gas pressure, provided that the surface loss probability is kept constant.

Considering the lifetimes of CF ($\sim$0.3 ms) and CF_2 ($\sim$5 ms) radicals,[22] the gas species in the chamber were mostly F and CF_4 in the late afterglow ($t\geqslant 25$ ms), where the F atom density decreased exponentially as shown in Fig. 3. Therefore, the dominant loss process of F atoms in the late afterglow may be the diffusion to the wall surface. The decay time constant τ_2 may correspond to the diffusion time constant τ_D, and the loss of F atoms due to reactions is negligible ($\tau_R\gg\tau_D$). If the reaction $F+F(+M)\rightarrow F_2(+M)$ is dominant, the decay curve of the F atom density is not approximated with an exponential function. The surface loss probability α is calculated by τ_2 and Eq. (5) as shown in Fig. 6. Since τ_2 is much longer than Λ_0^2/D, α can be evaluated from the second term of the right hand side of Eq. (5). The surface loss probability of F atoms was mainly on the order of 10^{-3}, and was strongly dependent on the CF_4 gas pressure.[25] This result suggests that the surface coverage (the fraction of sites covered with adsorbate) is greatly affected by the gas pressure.[26] According to the result, the surface coverage was an increasing function with the gas pressure, and was saturated at $\sim$10 mTorr. Note that the surface loss probability of CF_2 radicals obtained by the lifetime measurements with laser-induced fluorescence spectroscopy was on the order of 10^{-2}.[22]

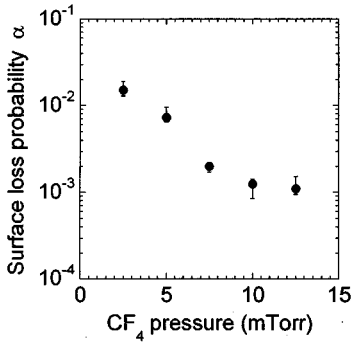

FIG. 6. The surface loss probability of F atoms corresponding to the decay time constant τ_2 shown in Fig. 5.

According to Eq. (4), the F atom density in the discharge plasma in the steady-state is given by

$$n_F=\tau k_p n_e n_{CF_4}. \tag{6}$$

The decay time constant τ_2 did not depend on the electron density so much when the CF_4 gas pressure was kept constant. According to Eq. (6), the constant lifetime should result in a proportional relation between n_F and n_e. However, a scaling law $n_F\propto n_e^{0.5\sim 0.7}$ was observed experimentally for fixed CF_4 gas pressures as shown in Fig. 2. Hence τ_2 does not correspond to the lifetime of F atoms in the discharge plasma. On the other hand, if we suppose that the decay time constant τ_1 in the initial afterglow represents the lifetime of F atoms in the discharge plasma ($\tau\simeq\tau_1$), the scaling laws shown in Eqs. (1) and (2) are roughly consistent with Eq. (6). The similar F atom density in spite of the longer τ_1 for the higher gas pressure can be attributed partly to the small production rate coefficient k_p in the high-pressure plasma because of the low electron temperature. In the discharge plasma, ionization $F+e\rightarrow F^+ +2e$ is also the loss process of F atoms. However, since the rate coefficient for the above reaction is 3.6×10^{-10} cm^3/s for an electron temperature of 5 eV,[14] the ionization loss cannot be dominant for the range of the electron density in the present experiments.

The duration of the initial decay of the F atom density roughly coincided with the lifetime of CF_2 radicals. Although we do not have any diagnostics for CF_3 radicals, the lifetime of CF_3 may be a similar value to that of CF_2.[27,28] Hence, the reason why the decay of the F atom density has two components can be attributed to the existence of CF_x ($x=2$ or 3) radicals in the chamber (the lifetime of CF radi-

cals was shorter than the duration of the initial density decay). When there are CF_x radicals in the chamber, they seem to be able to react with F atoms. If the reaction with CF_x radicals is fast enough to dominate the diffusion loss, the rapid density decay can be observed while the CF_x radicals survive in the chamber. In this period, the lifetime of F atoms satisfies the condition $\tau \simeq \tau_1 \simeq \tau_R \ll \tau_D$. However, according to the cross sectional data available to date, the reaction rate coefficients for the gas phase reactions between F and CF_x (such as $F+CF_x \rightarrow CF_{x+1}$ and $F+CF_x+M \rightarrow CF_{x+1}+M$) are too small to explain the short lifetime τ_1, since the gas pressures in the present experiments were low.[29] Hence, we propose the reaction (recombination) of F atoms with CF_x radicals on the wall surface,

$$F+CF_x \overset{\text{wall}}{\rightarrow} CF_{x+1}, \tag{7}$$

as the dominant loss process of F atoms in the discharge plasma and the initial afterglow. The importance of this reaction has been pointed out by Hikosaka and Sugai[8] as the loss process of CF_3 radicals. After the disappearance of the CF_x radicals, the major loss process of F atoms changes into the diffusion with a longer time constant.

Under the assumption described above, the lifetime τ_1 varies inversely as n_{CF_x} such that

$$\tau_1 \simeq \tau_R \propto \frac{1}{n_{CF_x}}. \tag{8}$$

This relationship is consistent with Eq. (2) when the density of CF_x radicals satisfies the following scaling law:

$$n_{CF_x} \propto (n_e n_{CF_4})^{(0.3-0.4)}. \tag{9}$$

The longer τ_1 for the higher gas pressure, as shown in Fig. 4, may be due to the decrease in the reaction rate coefficient for Eq. (7), which is partly determined by the surface conditions such as the coverage. Since the CF_2 radical density measured by laser-induced fluorescence spectroscopy was saturated (slightly decreased) for electron densities higher than $\sim 5\times 10^{11}$ cm^{-3},[19] the CF_2 radical density is not consistent with the scaling law shown in Eq. (9). Accordingly, the most probable species which reacts with F atoms is CF_3 radicals. If the reaction with CF_3 is the dominant loss process, the decrease in the F atom density during the initial afterglow roughly corresponds to the CF_3 radical density. According to the experimental results, the density drop during the initial afterglow increased with the rf power without saturation. For the example shown in Fig. 3, the density drop between $t=10$ ms and $t=14$ ms was $\sim 8.4\times 10^{12}$ cm^{-3}, which can be explained as the CF_3 density in the high-density helicon plasma with a gas pressure of 5 mTorr and an rf power of 1.5 kW.

V. CONCLUSION

In conclusion, we have shown the following:

(1) We carried out absolute density and lifetime measurements of F atoms in helicon-wave excited high-density CF_4 plasmas by using vacuum ultraviolet absorption spectroscopy.
(2) The F atom density in the discharge plasma was summarized as a function of the product between the electron and parent gas densities. As a result, a scaling law $n_F \propto (n_e n_{CF_4})^{(0.5-0.7)}$ was found.
(3) The decay of the F atom density in the afterglow was composed of two components with different time constants: the rapid decay in the initial afterglow and the exponential decrease in the late afterglow.
(4) The decay time constant τ_1 in the initial afterglow roughly satisfied the scaling law $\tau_1 \propto (n_e n_{CF_4})^{-(0.3-0.4)}$, which is a consistent relationship with the scaling law for the F atom density.
(5) The decay time constant τ_2 in the late afterglow was much longer than τ_1, and was strongly dependent on the CF_4 gas pressure. The surface loss probability of F atoms was evaluated from τ_2, and was mainly on the order of 10^{-3}.
(6) The above two scaling laws and the lifetimes of CF_x radicals suggest that the major loss process of F atoms in the discharge plasma and the initial afterglow is the reaction with CF_x radicals (probably, $x=3$) on the wall surface. In the late afterglow, the dominant loss process of F atoms is simple diffusion to the chamber wall.

ACKNOWLEDGMENTS

This work was supported by Tatematsu Foundation and by a Grant-in-Aid for Scientific Research from the Ministry of Education, Science, Sports, and Culture of Japan.

[1] R. A. H. Heinecke, Solid-State Electron. **18**, 1146 (1975).
[2] L. M. Ephrath and E. J. Petrillo, J. Electrochem. Soc. **129**, 2282 (1982).
[3] K. Suzuki, S. Okudaira, N. Sakudo, and I. Kanomata, Jpn. J. Appl. Phys., Part 1 **16**, 1979 (1977).
[4] G. S. Oehrlein, Y. Zhang, D. Vender, and O. Joubert, J. Vac. Sci. Technol. A **12**, 333 (1994).
[5] T. Fukasawa, K. Kubota, H. Shindo, and Y. Horiike, Jpn. J. Appl. Phys., Part 1 **33**, 7042 (1994).
[6] A. J. Perry, D. Vender, and W. Boswell, J. Vac. Sci. Technol. B **9**, 310 (1991).
[7] T. Tsukada, H. Nogami, Y. Nakagawa, and E. Wani, Jpn. J. Appl. Phys., Part 1 **33**, 4433 (1994).
[8] S. Samukawa, Jpn. J. Appl. Phys., Part 1 **33**, 2133 (1994).
[9] C. Suzuki and K. Kadota, Appl. Phys. Lett. **67**, 2569 (1995).
[10] M. Magane, N. Itabashi, N. Nishiwaki, T. Goto, C. Yamada, and E. Hirota, Jpn. J. Appl. Phys., Part 2 **29**, L829 (1990).
[11] H. Sugai and H. Toyoda, J. Vac. Sci. Technol. A **10**, 1192 (1992).
[12] J. W. Coburn and M. Chen, J. Appl. Phys. **51**, 3134 (1980).
[13] K. Sasaki, Y. Kawai, and K. Kadota, Appl. Phys. Lett. **70**, 1375 (1997).
[14] R. A. Bonham, Jpn. J. Appl. Phys., Part 1 **33**, 4157 (1994).
[15] D. Edelson and D. L. Flamm, J. Appl. Phys. **56**, 1522 (1984).
[16] T. Shoji, Y. Sakawa, S. Nakazawa, K. Kadota, and T. Sato, Plasma Sources Sci. Technol. **2**, 5 (1993).
[17] A. G. Mitchell and M. W. Zemansky, in *Resonance Radiation and Excited Atoms* (Cambridge University Press, Cambridge, 1961), p. 92.
[18] D. C. Morton, Astrophys. J., Suppl. Ser. **77**, 119 (1991).
[19] C. Suzuki, K. Sasaki, and K. Kadota, J. Appl. Phys. **82**, 5321 (1997).

[20] K. P. Shamrai and T. B. Taranov, Plasma Phys. Controlled Fusion **36**, 1719 (1994).
[21] K. Ura, K. Sasaki, and K. Kadota, J. Plasma Fusion Res. **72**, 1204 (1996).
[22] C. Suzuki, K. Sasaki, and K. Kadota, Jpn. J. Appl. Phys., Part 2 **36**, L824 (1997).
[23] P. J. Chantry, J. Appl. Phys. **62**, 1141 (1987).
[24] R. C. Reid, J. M. Prausnitz, and T. K. Sherwood, *The Properties of Gases and Liquids* (McGraw-Hill, New York, 1977).
[25] K. Sasaki, Y. Kawai, C. Suzuki, and K. Kadota, Abstracts of the 43rd National Symposium of American Vacuum Society, Philadelphia, 1996, p. 148.
[26] M. A. Lieberman and A. L. Lichtenberg, *Principles of Plasma Discharges and Material Processing* (Wiley, New York, 1994).
[27] L. D. Kiss and H. H. Sawin, Plasma Chem. Plasma Process. **12**, 523 (1992).
[28] Y. Hikosaka and H. Sugai, Jpn. J. Appl. Phys., Part 1 **32**, 3040 (1993).
[29] I. C. Plumb and K. R. Ryan, Plasma Chem. Plasma Process. **6**, 11 (1986).